

Received Date : 21-Jul-2016

Revised Date : 06-Nov-2016

Accepted Date : 02-Dec-2016

Article type : Original Manuscript

**Title Page**

Evaluation of the p-AKT, p-JNK and FoxO3a function in the oral epithelial dysplasia malignance.

**Running Head**

AKT, JNK and FoxO3a in oral epithelial dysplasia.

**Authors and name affiliations**

Filipe Nobre Chaves<sup>1</sup>, Thâmara Manoela Bezerra Marinho<sup>2</sup>, Paulo Goberlânio de Barros Silva<sup>2</sup>, Francisco Artur Forte Oliveira<sup>2</sup>, Fabrício Bitu Sousa<sup>2</sup>, Fábio Wildson Gurgel Costa<sup>2</sup>, Ana Paula Negreiros Nunes Alves<sup>2</sup>, Karuza Maria Alves Pereira<sup>1\*</sup>.

<sup>1</sup>School of Dentistry, Federal University of Ceara/Sobral, Sobral, Ceara, Brazil

<sup>2</sup>Department of Dental Clinic, Division of Oral Pathology, Faculty of Pharmacy, Dentistry and Nursing, Federal University of Ceara, Fortaleza, Ceara, Brazil

\*Correspondence author: PhD. MSc. DDS. Karuza Maria Alves Pereira

Federal University of Ceará campus Sobral

Rua Coronel Estanislau Frota, S/N – CEP 62.010-560, Centro, Sobral,  
Ceará

Phone 1/Fax Number: +55 (88) 3613-2603.

E-mail: karuzaalves@yahoo.com.br

This article has been accepted for publication and undergone full peer review but has not been through the copyediting, typesetting, pagination and proofreading process, which may lead to differences between this version and the Version of Record. Please cite this article as doi: 10.1111/odi.12623

This article is protected by copyright. All rights reserved.

## ABSTRACT

**OBJECTIVES:** To evaluate the expression of p-AKT, p-JNK, FoxO3a and KI-67 in samples of Oral Squamous Cell Carcinoma (OSCC) and Oral Epithelial Dysplasias (OEDs) to understand their possible involvement in the malignant transformation process of oral lesions. **MATERIALS AND METHODS:** Tissue samples of 20 cases of OSCCs, 20 OEDs and normal oral mucosa were subjected to immunohistochemistry reactions for anti-p-Akt, anti-p-JNK, anti-FoxO3a and anti-Ki-67 antibodies. It was analyzed quantitative (number of immunostained cells) and qualitative (immunostaining intensity) parameters in different cell immunostaining sublocations. **RESULTS:** Nuclear p-AKT was observed significantly greater immunostaining in OSCC ( $21.2 \pm 19.0$ ) than in dysplasias ( $7.9 \pm 8.1$ ) and control ( $1.8 \pm 4.7$ ) ( $p = 0.002$ ). Immunostaining of strong nuclear p-JNK was greater in controls ( $48.3 \pm 13.7$ ) than in OEDs ( $11.0 \pm 10.3$ ) and OSCCs ( $1.1 \pm 1.3$ ) ( $p < 0.001$ ). Strong nuclear immunostaining of FoxO3a proved to be absent in OSCCs ( $0.0 \pm 0.1$ ) with little staining on dysplasias ( $3.2 \pm 5.4$ ) and increased expression in controls ( $13.5 \pm 4.8$ ) ( $p < 0.001$ ). Immunostaining of strong nuclear ki-67 was greater in OSCCs ( $48.1 \pm 49.6$ ) than in OED ( $11.8 \pm 10.6$ ) and controls ( $1.9 \pm 2.0$ ) ( $p < 0.001$ ). **CONCLUSIONS:** Malignant process of OEDs in this research may involve the same mechanisms of established malignant lesions.

**KEYWORDS:** oral squamous cell carcinoma; oral epithelial dysplasia; immunohistochemistry; p-AKT; p-JNK; FoxO3a.

## INTRODUCTION

Oral Squamous Cell Carcinoma (OSCC) and pharyngeal cancer represent the sixth most common solid cancers around the world (Warnakulasuriya, 2009). Most patients with OSCC present with locally advanced disease and need multimodality therapy that may include surgery, radiotherapy, chemotherapy, and molecular therapy (Warnakulasuriya, 2009; Scully and Bagan, 2009). Thus, to understanding the molecular pathways of OSCC carcinogenesis and progression would be helpful in improving the diagnosis, therapy, and prevention of this disease (Scully and Bagan, 2009).

It is widely accepted that OSCC can arise from a premalignant lesion (LPM) (Scully and Bagan, 2009). However, not all LPMs become malignant, and oral epithelial dysplasia (OED) histopathology is an important predictor of malignancy (Warnakulasuriya *et al*, 2008; Scully and Bagan, 2009). Currently, the association between the degree of oral dysplasia and malignant transformation remains debatable (Warnakulasuriya *et al*, 2008). Additional study is therefore necessary to improve the histological grading of dysplasias. Furthermore, a better understanding of changes in molecular and biochemical processes in dysplasias may help identify specific biomarkers that, together with histological parameters, can lead to a more accurate diagnosis of the risk of malignant transformation of these lesions.

The PI3K / AKT signaling pathway is one of the most frequently deregulated pathways in cancer (Lam *et al*, 2006). The constant activation of this pathway in cancer is often a consequence of increased expression of genes that encode either class I PI3K (Phosphatidylinositol 3-Kinase) subunits (e.g., 110 $\alpha$ ) or AKT (protein kinase B), or is a result of genetic mutations that inhibit negative regulators of the PI3K / AKT pathway such as PTEN (phosphatase and tensin homologue) (Lam *et al*, 2006).

FoxO (forkhead box O) is a major target of p-AKT. Once it is phosphorylated, it loses its tumor suppressor function because it is translocated from the nucleus to the cytoplasm, induce cell death. P-AKT also reduces the ability of FoxO to bind to DNA and enhances its degradation. Cytoplasmic FoxO can be relocated to the nucleus by the presence of JNK (c-Jun N-terminal kinase), which is activated by stress, resulting in increased FoxO transcriptional activity (Lam *et al*, 2006). JNK is also responsible for phosphorylation of 14-3-3 chaperone proteins. This function results in the release of transcription factors linked to FoxO, as these proteins retain FoxO in the cytoplasm (Van der Heide *et al*, 2004; Lam *et al*, 2006). In OSCC, it has been suggested that FOXO3a activity can be important in malignant transformation and that tumor progression occurs through CDK4/6 and cyclin D1 inhibition, as well as p27 and Bim accumulation (Fang *et al*, 2011).

Genetic and epigenetic alterations occur during malignant transformation, but the prognostic meaning of the earliest genetic changes in malignancy remain unclear, as the progression of genetic damage over time has not yet been demonstrated (Warnakulasuriya *et al*, 2008). In addition, histopathology, even today, is the established method for assessing the risk of premalignant lesions, indicating the need for better models of biological risk (Massarelli *et al*, 2005). Given the above, the current study sought to understand the malignant transformation process of OEDs through the expression of biomarkers involved in the PI3K/AKT pathway using immunohistochemistry. Comparisons regarding the immunoreactivity of these biomarkers with OSCCs were also carried out.

## **MATERIALS AND METHODS**

This study consisted of an observational, analytical and cross-sectional study, using the diagnosis and immunomolecular analysis of malignant and premalignant lesions. We analysed 20 cases of OEDs, and 20 cases of OSCCs and 5 cases of normal oral epithelium (NOE). All samples were embedded in paraffin and obtained from incisional biopsies from patients of the Outpatient Stomatology Clinic of the Federal University of Ceará - Sobral Campus. Samples were collected from January 2012 to December 2015. The Research Ethics Committee of the Federal University of Ceara / Department of Clinical Medicine approved this clinical-laboratory study under protocol No 94432, and the written informed consent was obtained from all patients.

### ***Histomorphometric analysis***

Specimens were fixed in 10% formalin, embedded in paraffin, sectioned at 5 µm, stained with hematoxylin-eosin and mounted on glass slides for histopathological analysis.

OEDs specimens were classified using a binary low/high system of grading dysplasia for predicting malignant transformation (Warnakulasuriya *et al*, 2008). OSCCs specimens were categorized according to the WHO classification (Barnes *et al*, 2005).

The results of this classification were as follows: 10 were low risk of OEDs, 10 were high risk of OEDs, and 11 were well differentiated OSCCs and 9 were moderately differentiated OSCCs.

### ***Immunohistochemical Reaction***

For immunohistochemistry, 3-mm-thick sections were cut from paraffin-embedded material. All tissue samples were processed using standard methods, and serial sections were used for IHC. After deparaffinization and rehydration, slides were subjected to heat-induced epitope retrieval in 10 mmol/L citrate/trilogy buffer (pH=6.0) in a Pascall water bath (DakoCytomation). Endogenous peroxidase activity was blocked for 30 minutes with 0.3% hydrogen peroxide followed by 1% protein blocking for 10 minutes. The sections were incubated with primary antibodies describe in Table 1 (clone, manufacturer, dilution, antigen retrieval, and incubation). The samples were then incubated with the secondary antibody LSAB Kit (DAKO®, Carpentaria, CA, USA) for 10 minutes at room temperature. Next, development was performed using a chromogen solution prepared with DAB (3-3'-diaminobenzidine), for 10 minutes in a dark chamber (DAKO®, Carpentaria, CA, USA) and Harris hematoxylin was used for counterstaining.

Finally, coverslips were placed on the samples on glass slides, which were examined under a Leica DM 2000 optical microscope. A positive control was included in each reaction along with the samples. A negative control lacking primary antibody was performed in parallel with incubation of the experimental samples.

### ***Evaluation of IHC Staining***

The presence of brown color was used as the parameters for positive antigen labeling in all samples. Fields that were the highest signal (hot spots) were selected for imaging. Five fields were selected (adapted from Kruse-Losler *et al*, 2005), visualized and captured at 400x magnification with a Leica DFC295 HD digital camera using Las software at maximum resolution. Measurement of protein levels through conventional immunohistochemistry often cannot provide accurate results because the pathologist tends to group the immunoblots only as positive or negative. Furthermore, the use of cutoffs often impairs immunohistochemical analysis because values close to the cutoffs are still classified as “high” and “low” protein expressions (Yu *et al*, 2007). Thus, this study sought to not use scores in the analysis pattern.

Quantitative analysis of protein expression was performed by counting the number, in absolute values, of immunostained cells according to a methodology adapted from Vasconcelos *et al* (2015) and using Image J software (Image and Processing Analysis in Java – Rasband, W.S., ImageJ, National Institutes of Health, Bethesda, Maryland, USA). Two authors carried out the analysis at separate times while unaware of the clinical data, and any disagreement was resolved by discussion.

Qualitative analysis corresponded to the intensity of immunostaining, which was based on cells displaying no, weak, moderate or strong staining (Figure 1) at the appropriate locations (nucleus, perinucleus, cytoplasm or nuclear membrane) for each antibody according to methods adapted from previous studies (Mourão *et al*, 2016; Choi *et al*, 2005).

Qualitative and quantitative analyzes were performed simultaneously on each field. Analysis consisted of counting the number of positive cells in each field and quantifying the intensity of immunoblots of specific cellular locations for each antibody as previously described. The levels of each protein within cells were normalized and then assessed using statistical analysis as follows.

### **Statistical analysis**

Results of the above analyses were used to construct a database in an Excel spreadsheet. Then, this data was transferred to SPSS 17.0 running on a Windows system. The Kolmogorov-Smirnov normality testing was performed, and we utilized analysis of variance (ANOVA) followed by Bonferroni's post-test for comparisons between groups. The data were expressed as the mean and standard error of the mean (Mean $\pm$ s.e.m.) based on a 5% level of significance ( $p < 0.05$ ).

Previous data (Fillies *et al*, 2005; Ayala *et al*, 2010; Eckert *et al*, 2011) were also used in order to meet the appropriate requirements for statistical analysis, and the sample size was calculated. The sample was been designed to provide a power of 80% and a confidence level of 95% to detect a significant differences in immunohistochemical results between the groups of patients with oral lesions. Additionally, the sample was designed to sustain a 20% loss, resulting in a final sample estimated to include 20 patients.

## **RESULTS**

### *p*-JNK

Immunohistochemical analysis of p-JNK revealed nuclear and cytoplasmic immunostaining in both normal and dysplastic epidermoid cells of all evaluated specimens (Figure 1).

The average number of cells with strong nuclear immunostaining was higher in controls compared to OED and OSCC samples ( $p < 0.001$ ). Conversely, the highest average number of cells with weak nuclear immunostaining was observed in OSCC samples ( $p < 0.001$ ). There was no difference between the average intensity of cytoplasmic immunostaining (Table 2), nor was a difference in nuclear staining observed between the different gradations of OED (Table 3).

There was no difference in nuclear and cytoplasmic p-JNK staining between the different sets of OSCC. Nevertheless, nuclear staining was highest in the OSCC groups, followed by OED and then the control group ( $p < 0.001$ ). These results indicate an inverse association between the level of p-JNK in the nucleus and the degree of tissue dysplasia (Table 3).

### *FoxO3a*

Immunohistochemical analysis of FoxO3a revealed nuclear and cytoplasmic signal in both normal and dysplastic cells of all evaluated specimens (Figure 1).

A higher average number of cells with nuclear immunostaining was found in NOE compared to OED and OSCC ( $p < 0.001$ ). Most of this signal was strong ( $p < 0.001$ ) and moderate ( $p < 0.001$ ) (Table 2). We also observed a difference in nuclear signal between different gradations of OED ( $p = 0.010$ ), with greater numbers of cells showing weak cytoplasmic signal in low risk OED ( $p = 0.029$ ) (Table 3).

As seen in Table 4, we observed a difference in cytoplasmic immunostaining between high and low risk OSCC and OED ( $p = 0.040$ ), with a higher level of staining in OSCC. This difference is better evidenced in cells displaying weak cytoplasm immunostaining, where a higher average number was observed in OSCC compared to NOE and HRD ( $p = 0,001$ ), and in cells with moderate cytoplasm immunostaining, where a higher average number was observed in OSCC compared to low risk OED ( $p = 0.019$ ).

### *p-AKT*

Immunohistochemical analysis of p-AKT revealed nuclear, perinuclear and cytoplasmic immunostaining in the dysplastic epidermoid cells of all evaluated specimens. Membrane staining was not observed in NOE (Figure 1).

We observed increased nuclear staining in OSCC compared to NOE and OED ( $p = 0.002$ ). A similar pattern was found for weak cytoplasmic immunostaining, where more OSCC cells displayed low cytoplasmic signal relative to the other groups ( $p < 0.001$ ). OED samples displayed greater numbers of cells with strong and moderate cytoplasmic immunostaining relative to OSCC samples ( $p=0.022$  and  $0.002$ , respectively). Regarding membrane marking, immunostaining was higher in OSCC compared to OED and NOE ( $p < 0.001$ ) (Table 2). There was a difference in strong and moderate membrane labeling between the gradations of OED ( $p = 0.022$  and  $0.002$ , respectively) (Table 3).

As shown in Table 4, we observed greater perinuclear signal in low risk OED compared to OSCC ( $p = 0.029$ ). We also observed membrane signal that increased with the degree of malignant differentiation ( $p < 0.001$ ), and correlated inversely to weak cytoplasmic signal ( $p < 0.001$ ). Interestingly, there was a greater level of moderate membrane staining in high risk OED samples compared to low risk OED and control samples ( $0 \pm 0$ ) ( $p < 0.001$ ). Finally, greater levels of strong membrane signal in OSCC samples relative to controls was observed ( $p = 0.008$ ).

### *KI-67*

Analysis of Ki-67 revealed exclusive nuclear (nucleoplasm and nucleolus) immunostaining in both normal and dysplastic epidermoid cells of all evaluated specimens, with greater signal in the basal and parabasal layers of control samples (Figure 1).

The mean number of cells displaying nuclear Ki-67 was directly linked to the grade of cell differentiation ( $p < 0.001$ ), regardless of whether the signal was strong, moderate, or low staining ( $p < 0.001$ ) (Table 2). There was no difference in nuclear staining between the gradations of OED and OSCC (Table 3). The average number of cells positive for Ki-67 was increased most significantly

increased in the OSCC groups, followed by HRD, LRD and control groups ( $p < 0.001$ ). This association was further confirmed by stronger nuclear staining in OSCC compared with low-risk and control OED ( $p = 0.001$ ). Moderate staining was greater in OSCC compared to OED and controls ( $p < 0.001$ ). Finally, mild staining was greater in OSCC and HRD compared to the controls ( $p < 0.001$ ) (Table 4).

### *Correlations*

To determine the possible interactions between the molecules studied and to better understand their functions and mechanisms of action in the OEDs and OSCCs, we built a diagram that shows a covariance structure model of the antitumor antibodies FoxO3a and p-JNK, as well as KI-67 activation influenced by AKT in the cases of OSCC (Figure 2) and OED samples (Figure 3) of this research. The analyzed data were then further assessed using Pearson Correlation Test.

## **DISCUSSION**

This immunohistochemical study was designed to understand and relate the carcinogenesis of OED and OSCC through the PI3K/AKT signaling pathway, which has been extensively investigated in the tumorigenesis process of multiple types of cancers, including OSCCs. However, few studies have approached the association of potentially malignant oral lesions with deregulation of this pathway.

### *p-JNK*

In the samples we examined, specimens with dysplasia showed similar behavior to OSCC cases, with loss of nuclear p-JNK (Table 2). Nuclear p-JNK localization appears to be lost in the malignant lesion, as there were more cells with strong nuclear immunostaining in low-grade dysplasia compared to high grade (Table 3). These findings lead us to assume that the lower nuclear levels of p-JNK in these samples are related to the regulation of tumorigenesis. Similar research using human gastric cancer specimens found greater nuclear staining of p-JNK during early clinical stages of the tumor, in patients with higher survival rates, and correlated inversely with lymphatic invasion (Choi *et al*, 2016). Despite these findings suggesting a protective role of p-JNK, Choi *et al* (2016) found, through cell culture experiments, that the inhibition of p-JNK reduced the expression of D1 cyclin proteins and limited colony formation. This indicated that the activation of p-JNK (Nuclear JNK) is at least partially required for cell growth and proliferation in the early stages of cancer. However, we must consider that p-JNK does not have a single target, such as cyclins, but a large number of downstream substrates that are mostly nuclear transcription factors, cytoplasmic proteins and the mitochondrial membrane proteins (Wang *et al*, 2012). The tumor suppressor activity of JNK is closely related to its apoptotic function through a mitochondrial pathway (Davis, 2000), which can occur when p-JNK targets p53 by promoting its phosphorylation and subsequent accumulation and activation as a transcriptional regulator (Oleinik *et al*, 2007).

In this study, we did not observe differences in the p-JNK expression patterns in HRD and OSCC (Table 4), which led us to believe that malignant transformation of dysplasias may involve the same mechanisms of established malignant lesions. One possible explanation of this finding is that the cell has a fail-safe mechanism, which requires coordinated activity between JNK and P53 (Gowda *et al*, 2012). As P53 is often lost in OSCC and OEDs, the apoptosis may therefore not be induced by p-JNK, contributing to the oncogenic cellular transformation. This study did not conduct experiments with P53, which limited us to draw only theories to explain our results and not make greater conjectures. Further research seeking to analyze the crosstalk between P53 and p-JNK in the carcinogenesis process are therefore necessary.

Findings from previous work have demonstrated aberrant expression of JNK in many cancer cell lines, as well as in biopsy samples from cancer patients (Hui *et al*, 2008; Chang *et al*, 2009; Barbarulo *et al*, 2013). This suggests that JNK may contribute to the cellular transformation required for carcinogenesis (Bubici and Papa, 2014), as the individual depletion of various subtypes of JNKs can suppress tumor activity depending on the specificity of the tissue (Wagner and Nebreda, 2009). The pro-tumorigenic role of JNK in many types of cancer has led to increasing investigation into possible therapeutic avenues using this protein. However, inhibition of JNK can also be harmful (Bubici and Papa, 2014), as substantial evidence has implicated JNK as a tumor suppressor (Davis, 2000; Wagner and Nebreda, 2009). Thus, it is necessary to understand the molecular basis of the dual role of JNK in different tumors in order to validate the actual therapeutic potential of inhibiting it (Bubici and Papa, 2014). One possible explanation for the opposing pro- and anti-tumorigenic roles of JNK is the regulation of many specific cellular targets in different cancer types, although many of these target proteins remain still unknown (Bubici and Papa, 2014). Other variables that affect the level of complexity of JNK regulation in tumorigenesis include the stimulus for activation, duration of activation and the context of its production (Du *et al*, 2004).

### *FoxO3a*

Here, we observed that the advance of malignance in dysplasias was accompanied by the gradual loss of nuclear FoxO3a immunostaining (Table 3), leading to similar qualitative immunostaining results as those observed in HRD and OSCCs (Table 4). The antitumor role of FoxO3a in OSCC has been previously demonstrated (Fang *et al*, 2011a, Fang *et al* 2011b, Chi *et al*, 2015). Its nuclear localization is associated with decreased cell proliferation and increased apoptosis of tumor cells *in vitro*, as well decreased tumor size *in vivo* (Fang *et al*, 2011b). Together with the results of the current work, these results suggest that the loss of nuclear FoxO3a is involved not only in established malignant lesions but also in the malignant transformation of oral dysplasia. To our knowledge, this is the first study that evaluates FoxO3a in the context of oral dysplasias.

However, recent research has shown an unexpected pro-tumorigenic role of FoxO, suggesting more complex activity of this protein in tumors (Hui *et al*, 2008, Tenbaum *et al*, 2012, Osuka *et al*, 2013, Yu *et al*, 2016). Here, through the analysis of FoxO3a expression *in situ*, we found no evidence of a possible pro-tumorigenic role of this protein in the samples examined. Previous work has demonstrated that in the early stages of a tumor, inactivating FoxO3a provides a proliferative advantage to neoplastic cells by increasing signaling through



growth factor. In contrast, the later stages of tumor stress conditions, such as serum deprivation, hypoxia and oxidative stress, can reactivate FoxO3a and thus increase the survival of tumor cells (Li *et al*, 2012; Yu *et al*, 2016). These data underpin the findings of the present study, allowing us to propose that the inactivation of FoxO3a in dysplasias (i.e., early-stage malignant lesions), contributes in some way to their malignant progression. Furthermore, the inactivation of FoxO3a provides a proliferative advantage to OSCCs investigated in this study. Our samples were in the early stages of malignancy, as the sample was composed only of well differentiated and moderately differentiated tumours, with no poorly differentiated cases. Thus, the role of FoxO3a in tumorigenesis is context-dependent (Li *et al*, 2012), as its activity is controlled differently in specific tissues in response to various external stimuli and intensities (Calnan and Brunet, 2008).

We observed a significant increase in weak cytoplasmic immunostaining in the OSCCs group relative to the HRD group (Table 4). This may be due to a certain degree of protein degradation because FoxO can be ubiquitinated and degraded by cytoplasm proteasomes (Van der Heide *et al*, 2004). In this study, cytoplasmic immunostaining of FoxO3a near the membrane was observed both in the control group and in the dysplasias and OSCC samples; however, this parameter was not measured.

#### *p-AKT*

The activity of Akt is modulated downstream of PI3K, and then the protein is recruited to the sites of plasma membrane and phosphorylated at two sites by PDK1 (phosphoinositide-dependent kinase 1) (at Thr308, AKT1 residue) and mTORC2 (mammalian target of rapamycin) (Ser473, residue AKT1) (Nicholson and Anders, 2002; Dillon and Muller, 2010). This leads to AKT activation, where phosphorylated AKT dissociates from the plasma membrane and phosphorylates its targets in the cytoplasm and nucleus (Dillon and Muller, 2010). The phosphorylation of these AKT targets is required for oncogenic transformation (Mende *et al*, 2001). However, the selection of the substrate can be affected by AKT localization within the cell location (Dufner *et al*, 1999), so it is therefore important to know the subcellular localization of this protein (Nicholson and Anders, 2002). Our current study assessed the immunostaining of p-AKT at the membrane, cytoplasm, nucleus and perinuclear regions. To our knowledge, this is the first study to evaluate activated AKT activated in the context of all levels of cellular location.

AKT1 does not efficiently transform cells in culture unless it is bound to the plasma membrane (Mirza *et al*, 2000; Sun *et al*, 2001). Thus, pathological association of AKT with the plasma membrane is a common thread that connects AKT with cancer (Carpten *et al*, 2007). Here, we observed that the presence of p-AKT at the membrane was proportional to the degree of malignancy of the dysplasia (Table 3). This results gives us reason to believe that the malignant transformation process of oral lesions and oral cancer involves the AKT1 activation, and that activation of this protein is essential in the early stages of malignant transformation of oral lesions.

Interestingly, when analysing the intensity of immunostaining, we observed that the OSCC samples had a pattern of weak membrane immunostaining that was significantly higher than that seen in HRD and LRD. We also observed light cytoplasmic immunostaining that was significantly higher in OSCC than in HRD and the controls (Table 4). This result could be due to

AKT nuclear translocation, as this is part of its activation process (Noguchi *et al*, 2014) and leads to reduction of Akt levels at the plasma membrane and in the cytoplasm (Dillon and Muller, 2010). In addition, the most sensitive mechanism to reduce AKT activity is autophagy (Degtyarev *et al*, 2008). This finding leads us to suggest that the lower expression of AKT at the membrane and in the cytoplasmic found in this study might also be related to the induction of autophagy.

Autophagy has been implicated both in tumor suppression (Takamura *et al*, 2011; White *et al*, 2012) as well as in promoting tumor growth (White *et al*, 2012). The activation of AKT in the plasmatic membrane analysed inhibits the autophagy induction and the AKT at the plasma membrane inhibits induction of autophagy, and translocation of AKT from the cytosol to lysosomes induces autophagy (Noguchi *et al*, 2014; Matsuda-Lennikov *et al*, 2014). AKT1 and AKT2, but not AKT3, interact with the lysosomal protein Phafin2 (also known as EAPF or PLEKHF2). Furthermore, AKT-Phafin2 translocation to the perinuclear lysosomes has been implicated in autophagy (Noguchi *et al*, 2014; Matsuda-Lennikov *et al*, 2014). The perinuclear immunostaining of p-Akt in this study was found to be significantly higher in the LRD samples than in OSCCs (Table 4). It was also significantly higher in LRD when compared to HRD (Table 3), suggesting the involvement of autophagolysosomes in inhibiting the PI3K-AKT pathway in the early stages of progression of malignancy. The lower cytoplasmic and membrane levels of p-AKT we found in OSCC may contribute to autophagy; however, no statistically significant in these levels were observed when compared to the control group (Table 4). This may be explained because in the present study, despite presenting data related to the pathological staging of OSCC, the choice of these cases may have been biased towards selection of lesions in early clinical stages, as we had limited access to the clinical assessments of the cases studied. Moreover, contrary to the methodology of Massarelli *et al* (2005), case controls in our current study did not exclude smoking and/or alcohol consumption. This may have influenced the immunohistochemical results, as previous cell culture experiments have shown that AKT activation occurs within a few minutes of when cells are exposed to cigarette substances in concentrations similar to those occurring in the individual smoker (West *et al*, 2002).

#### Ki-67

Immunostaining with Ki-67 antibodies is well established as a quick and efficient method to evaluate the antiproliferative profile of neoplasias, as the protein binds to cells undergoing proliferation (Birajdar *et al*, 2014). In this study, Ki-67 immunohistochemical analysis revealed the protein exclusively in the nuclei of OSCC and OED cells, while in controls it was observed more commonly at the basal and parabasal layers. These findings corroborate the studies of Kobayashi *et al* (2010) and Hasegawa *et al* (2016), who suggested this protein as an important marker in the histopathologic scope of premalignant epithelial lesions. The presence of nuclear Ki-67 was significantly increased in OSCC compared to OED and the control (Table 2). It was also greater in OED samples compared to the control, revealing a direct relationship between KI-67 immunoreactivity and the grade of malignant cell differentiation and proliferation (Birajdar *et al*, 2014; Hasegawa *et al*, 2016).

Birajdar *et al* (2014) reported that immunostaining for Ki-67 increases with proliferative cellular activity and OED degree, suggesting this protein as an important marker of for proliferation and for sorting / grading in the OED based on greater expression in the suprabasal layers. In this study, we noted the same trend in the samples; however, Ki-67 expression did not differ between HRD and LRD (Table 3), regardless of the localization pattern. These findings lead us to believe that the lower level of Ki-67 seen in OED can be related to the state of proliferation and differentiation of OED. Kujan *et al* (2006) analysed immunostaining of Ki-67 in HRD and LRD. The authors found lower levels in the basal, stratum spinosum and parabasal cell layers in LRD samples, while in the number of proliferating cells with positive staining for Ki-67 was higher in HDR, consistent with the degree of dysplasia.

This increased proliferation in parabasal layers of OED is probably related to loss of heterozygosity in 3p, 9p, and 17p, which serve a markers of differentiation, and increases the risk of neoplasias (Tabor *et al*, 2003; Birajdar *et al*, 2014).

As seen in Figure 2, we observed that the presence of cytoplasmic AKT in OSCC was moderately but directly correlated with its membrane form. These findings are in agreement with the literature, as AKT activation begins at the membrane and carries out its various functions upon reaching the cytoplasm where it targets diverse substrates (Nicholson and Anderson, 2002; Gonzalez and McGraw, 2009; Dillon and Muller, 2010). Interestingly, we did not observe this association in OED samples (Figure 2), which leads us to suggest that the activation of AKT in these injuries could happen through a mechanism that does not involve the classic mode of AKT activation; that is, through its prior activation at the membrane. Recent studies have demonstrated that other kinases can interact with AKT and induce cellular transformation without requiring the PI3K signaling pathway (Mahajan *et al*, 2010; Joung *et al*, 2011; Xie *et al*, 2011; Guo *et al*, 2011; Mahajan and Mahajan 2012). Ser / Thr kinase I- $\kappa$ -B kinase epsilon (I $\kappa$ BE) has the ability to activate AKT regardless of the PH domain and without requiring PI3K, mTORC2, or PDK1 (Xie *et al*, 2011; Guo *et al*, 2011). The non-receptor tyrosine kinase Ack I (activated CDC42-associated kinase 1) is able to recruit and activate AKT by inducing the phosphorylation of Tyr176 residue without necessitating PI3K activity (Mahajan *et al*, 2010). Additionally, TBK1 (TANK-binding kinase I) interacts with and activates AKT in a PI3K-independent manner (Joung *et al*, 2011). Other kinases involved in this pathway include protein kinase 6, Src (cellular Src kinase), DNA-PK (DNA-dependent protein kinase) and ATM (ataxia telangiectasia mutated protein) (Mahajan and Mahajan 2012).

As previously discussed, we found here that autophagy, denoted by the presence of perinuclear AKT (Matsuda-Lennikov *et al*, 2014; Noguchi *et al*, 2014), was primarily observed in OED (especially in LRD) rather than in the OSCC. Interestingly, Figure 2 shows that in OSCC, the cell autophagy process is directly related to increased cell proliferation, represented by immunostaining of KI-67. This finding leads us to suggest a different role for autophagy in OSCC compared to that observed in OED, and it emphasizes that cell autophagy is context dependent (White *et al*, 2012). Similar research has found a direct association between markers related to autophagy and Ki-67 in breast cancer samples (Ueno *et al*, 2016). A link between nuclear AKT and greater cell proliferation rates is expected, as AKT targets certain nuclear substrates and its nuclear localization is a requirement for activation (Noguchi *et al*, 2014). The presence of nuclear p-AKT was found during similar studies of oropharyngeal squamous cell cancer, revealing a significant inverse correlation with the immunoexpression of nuclear PTEN (Yu *et al*, 2007).

Nuclear AKT immunostaining provided a strong and direct correlation with cytoplasmic JNK (Figure 2). A direct connection between JNK and the AKT pathway has not been found (Kim *et al*, 2001). However, the association between JNK and AKT appears to involve cross-talk with FoxO3a, as previously discussed. Furthermore, increased AKT activity may lead to suppression of the apoptotic activity of JNK (Kim *et al*, 2001; Fey *et al*, 2012), allowing its activity to be only proliferative (Fey *et al*, 2012). Kim *et al* (2001) found that Akt suppresses apoptotic activity of JNK through phosphorylation and subsequent inactivation of ASK1 (signal-regulating kinase 1), which is responsible for activating MKK4 (mitogen-activated protein kinase kinase 4) and MKK7 (mitogen-activated protein kinase kinase 7). The latter proteins are directly involved in activation of JNK. As previously discussed, we assume that in the tumor context of OSCC used here, nuclear AKT may be heavily involved in the relocation of JNK to the cytoplasm, thereby preventing it from acting on nuclear transcription factors that may have tumor suppressor role.

As show Figure 3, we observed in OEDs a weak inverse correlation between the presence of membrane and nuclear AKT. As previously discussed, the nuclear translocation of AKT reduces its levels at the membrane and in the cytoplasm, affecting the phosphorylation of substrates in these cellular compartments (Dillon and Muller, 2010). Nuclear translocation also increases its influence on specific nuclear targets, generating, among other things, progression of the cell cycle and suppression of apoptosis (Martelli *et al*, 2012). Despite not knowing exactly how AKT enters the nucleus (Martelli *et al*, 2012), it is important to note here is we identified its nuclear localization in OEDs and in OSCCs, with statistically significant differences between the two (Table 2). The presence of nuclear AKT is found in several types of cancer, such as lung (Lee *et al*, 2002), breast (Nicholson *et al*, 2003), thyroid (Vasko *et al*, 2004), prostate (Van de Sande *et al*, 2005) and invasive cellular carcinomas of the head and neck (Giudice *et al*, 2011). Here, we also found nuclear AKT in premalignant lesions in this study, which leads us to suggest that AKT in the nucleus is involved in the process of malignant transformation cell.

Cytoplasmic localization of JNK had a moderate inverse correlation with perinuclear localization of AKT (Figure 3). As previously noted, although a direct connection between AKT and JNK has not yet been found (Kim *et al*, 2001), we can suggest based on this finding that the process of cellular autophagy, indicated by the presence of AKT perinuclear (Matsuda-Lennikov *et al*, 2014; Noguchi *et al*, 2014), is connected with the reduction of cytoplasmic JNK. Zhou *et al* (2015) previously warned about the need to investigate the crosstalk between the JNK pathway and other autophagic signaling pathways. Additional research has found that cytoplasmic and nuclear JNK are involved in cell autophagy (Mehrpour *et al*, 2010). However, according to Zhou *et al* (2015), the JNK signalling pathway is extremely complicated and little is known about its role in autophagy.

Membrane localization of AKT was moderately inversely correlated with the presence of nuclear FoxO3a (Figure 3). These results are consistent with those reported in the literature, as the phosphorylation and subsequent activation of AKT results in the sequestration of FoxO away from the nucleus in the cytoplasm (Van der Heide *et al*, 2004). Thus, as seen in the present work, the loss of nuclear FoxO3a and with its subsequent relocation to the cytoplasm shows a process involved in the malignant transformation of the OED.

In conclusion, we emphasize that this study has limitations because it is based solely on immunohistochemistry, and this technique can only assess protein expression and not the mRNA. However, using this method, we conclude that the malignant transformation process of

the OED investigated here may involve the same mechanisms as established malignant lesions. Furthermore, the cellular localization of the proteins investigated has a direct role in their functions within the tumor microenvironment. This is especially true for the antitumorigenic activity of p-JNK and FoxO3a in both OEDs and OSCCs. Lastly, we found autophagy to be dependent on the context, based on a direct correlation between autophagy and cell proliferation only in cases of OSCC. This allowed us to conclude that, in these cases, autophagy has a pro-tumorigenic role.

#### ACKNOWLEDGMENT

This work was supported by grants from Conselho Nacional de Desenvolvimento Científico e Tecnológico (CNPq), Brazil. The authors would like to acknowledge Programa de Pós-Graduação em Odontologia da Universidade Federal do Ceará, Brazil.

#### REFERENCES

Ayala FR, Rocha RM, Carvalho KC, Carvalho AL, da Cunha IW, Lourenco SV, et al (2010). GLUT1 and GLUT3 as potential prognostic markers for Oral Squamous Cell Carcinoma. *Molecules* **15**: 2374-87.

Barbarulo A, Iansante V, Chaidos A, Naresh K, Rahemtulla A, Franzoso G, Karadimitris A, Haskard DO, Papa S, Bubici C (2013). Poly(ADP-ribose) polymerase family member 14 (PARP14) is a novel effector of the JNK2-dependent pro-survival signal in multiple myeloma. *Oncogene* **32**:4231-42.

Barnes L, Eveson J, Reichart P, Sidransky D (2005). World Health Organization classification of tumours. Pathology and genetics of head and neck tumours. IARC, Lyon. pp 209–253.

Birajdar SS, Radhika MB, Paremala K, Sudhakara M, Soumya M, Gadivan M (2014). Expression of Ki- 67 in normal oral epithelium, leukoplakic oral epithelium and oral squamous cell carcinoma. *Journal of Oral and Maxillofacial Pathology* **18**: 169-176.

Bubici C, Papa S (2014). JNK signalling in cancer: in need of new, smarter therapeutic targets. *British journal of pharmacology* **171**: 24-37.

Calnan DR, Brunet A (2008). The FoxO code. *Oncogene* **27**: 2276-88.

Carpten JD, Faber AL, Horn C, Donoho GP, Briggs SL, Robbins CM, et al (2007). A transforming mutation in the pleckstrin homology domain of AKT1 in cancer. *Nature* **448**: 439-44.

Chang CJ, Mulholland DJ, Valamehr B, Mosessian S, Sellers WR, Wu H (2008). PTEN nuclear localization is regulated by oxidative stress and mediates p53-dependent tumor suppression. *Molecular and cellular biology* **28**: 3281-9.

Chang Q, Zhang Y, Beezhold KJ, Bhatia D, Zhao H, Chen J, et al (2009). Sustained JNK1 activation is associated with altered histone H3 methylations in human liver cancer. *Journal of hepatology* **50**: 323-33.

Chang Y, Wu XY (2009). The role of c-Jun N-terminal kinases 1/2 in transforming growth factor beta(1)-induced expression of connective tissue growth factor and scar formation in the cornea. *The Journal of international medical research* **37**: 727-36.

Choi BY, Choi HS, Ko K, Cho YY, Zhu F, Kang BS, Ermakova SP, Ma WY, Bode AM, Dong Z. (2005). The tumor suppressor p16(INK4a) prevents cell transformation through inhibition of c-Jun phosphorylation and AP-1 activity. *Nature structural & molecular biology* **12**: 699-707.

Choi Y, Park J, Choi Y, Ko YS, Yu DA, Kim Y, Pyo JS, Jang BG, Kim MA, Kim WH, Lee B. (2016). c-Jun N-terminal kinase activation has a prognostic implication and is negatively associated with FOXO1 activation in gastric cancer. *BMC gastroenterology* **16**: 59.

Davis RJ (2000). Signal transduction by the JNK group of MAP kinases. *Cell* **103**: 239-52.

Degtyarev M, De Maziere A, Orr C, Lin J, Lee BB, Tien JY, Prior WW, van Dijk S, Wu H, Gray DC, Davis DP, Stern HM, Murray LJ, Hoeflich KP, Klumperman J, Friedman LS, Lin K (2008). Akt inhibition promotes autophagy and sensitizes PTEN-null tumors to lysosomotropic agents. *The Journal of cell biology* **183**: 101-16.

Dillon RL, Muller WJ (2010). Distinct biological roles for the akt family in mammary tumor progression. *Cancer research* **70**: 4260-4.

Du L, Lyle CS, Obey TB, Gaarde WA, Muir JA, Bennett BL, Chambers TC (2004). Inhibition of cell proliferation and cell cycle progression by specific inhibition of basal JNK activity:

evidence that mitotic Bcl-2 phosphorylation is JNK-independent. *The Journal of biological chemistry* **279**: 11957-66.

Dufner A, Andjelkovic M, Burgering BM, Hemmings BA, Thomas G (1999). Protein kinase B localization and activation differentially affect S6 kinase 1 activity and eukaryotic translation initiation factor 4E-binding protein 1 phosphorylation. *Molecular and cellular biology* **19**: 4525-34.

Eckert AW, Lautner MH, Schutze A, Taubert H, Schubert J, Bilkenroth U (2011). Coexpression of hypoxia-inducible factor-1alpha and glucose transporter-1 is associated with poor prognosis in oral squamous cell carcinoma patients. *Histopathology* **58**: 1136-47.

Fey D, Croucher DR, Kolch W, Kholodenko BN (2012). Crosstalk and signaling switches in mitogen-activated protein kinase cascades. *Front Physiol* **3**: 355.

Fillies T, Werkmeister R, van Diest PJ, Brandt B, Joos U, Buerger H (2005). HIF1-alpha overexpression indicates a good prognosis in early stage squamous cell carcinomas of the oral floor. *BMC cancer* **5**: 84.

Giudice FS, Dal Vecchio AMD, Abrahao AC, Sperandio FF, Pinto DD (2011) Different expression patterns of pAkt, NF- $\kappa$ B and cyclin D1 proteins during the invasion process of head and neck squamous cell carcinoma: an in vitro approach. *J Oral Pathol Med* **40**: 405-411.

Gowda PS, Zhou F, Chadwell LV, McEwen DG (2012). p53 binding prevents phosphatase-mediated inactivation of diphosphorylated c-Jun N-terminal kinase. *The Journal of biological chemistry* **287**: 17554-67.

Guo JP, Coppola D, Cheng JQ (2011). IKBKE protein activates Akt independent of phosphatidylinositol 3-kinase/PDK1/mTORC2 and the pleckstrin homology domain to sustain malignant transformation. *J Biol Chem* **286**: 37389-37398.

Hasegawaa M, Cheng J, Maruyama S, Yamazaki M, Abéa T, Babkair H, Saito C, Saku T (2016). Differential immunohistochemical expression profiles of perlecan-binding growth factors in epithelial dysplasia, carcinoma in situ, and squamous cell carcinoma of the oral mucosa. *Research and Practice* **212**: 426-436

Hui L, Zatloukal K, Scheuch H, Stepniak E, Wagner EF (2008). Proliferation of human HCC cells and chemically induced mouse liver cancers requires JNK1-dependent p21 downregulation. *The Journal of clinical investigation* **118**: 3943-53.

Joung SM, Park ZY, Rani S, Takeuchi O, Akira S, Lee JY (2011). Akt contributes to activation of the TRIF-dependent signaling pathways of TLRs by interacting with TANK-binding kinase 1. *J Immunol* **186**: 499-507.

Kim DK, Cho ES, Seong JK, Um HD (2001). Adaptive concentrations of hydrogen peroxide suppress cell death by blocking the activation of SAPK/JNK pathway. *J Cell Sci* **114**: 4329-34.

Kobayashi T, Maruyama S, Cheng J, Ida-Yonemochi H, Yagi M, Takagi R, Saku T (2010). Histopathological varieties of oral carcinoma in situ: diagnosis aided by immunohistochemistry dealing with the second basal cell layer as the proliferating center of oral mucosal epithelia, *Pathol Int* **60**: 156-166

Kruse-Lösler B, Flören C, Stratmann U, Joos U, Meyer U (2005). Histologic, histomorphometric and immunohistologic changes of the gingival tissues immediately following mandibular osteodistraktion. *J Clin Periodontol* **32**: 98-103.

Kujan O, Oliver RJ, Khattab A, Roberts SA, Thakker N, Solan P (2006). Evaluation of a new binary system of grading oral epithelial dysplasia for prediction of malignant transformation. *Oral Oncol* **42**: 987- 93.

Lam EW, Francis RE, Petkovic M (2006). FOXO transcription factors: key regulators of cell fate. *Biochemical Society Transactions* **34**: 722-6.

Lee SH, Kim HS, Park WS, Kim SY, Lee KY, Kim SH, Lee JY, Yoo NJ (2002). Non-small cell lung cancers frequently express phosphorylated Akt; an immunohistochemical study. *APMIS* **110**: 587-592.

Li Z, Zhang H, Chen Y, Fan L, Fang J (2012). Forkhead transcription factor FOXO3a protein activates nuclear factor kappaB through B-cell lymphoma/leukemia 10 (BCL10) protein and



promotes tumor cell survival in serum deprivation. *The Journal of biological chemistry* **287**: 17737-45.

Liu W, Shi LJ, Wu L, Feng JQ, Yang X, Li J, Zhou ZT, Zhang CP (2012). Oral cancer development in patients with leukoplakia--clinicopathological factors affecting outcome. *PloS one* **7**: e34773.

Mahajan K, Coppola D, Challa S, Fang B, Chen YA, Zhu W, Lopez AS, Koomen J, Engelman RW, Rivera C, Muraoka-Cook RS, Cheng JQ, Schönbrunn E, Sebti SM, Earp HS, Mahajan NP (2010). Ack1 mediated AKT/PKB tyrosine 176 phosphorylation regulates its activation. *PLoS ONE* **5**: e9646.

Mahajan K, Mahajan NP (2012). PI3K-independent AKT activation in cancers: A treasure trove for novel therapeutics. *J Cell Physiol* **227**: 3178–3184.

Martelli AM, Tabellini G, Bressanin D, Ognibene A, Goto K, Cocco L, Evangelisti C (2012). The emerging multiple roles of nuclear Akt. *Biochim Biophys Acta* **1823**: 2168-78.

Massarelli E, Liu DD, Lee JJ, El-Naggar AK, Lo Muzio L, Staibano S, De Placido S, Myers JN, Papadimitrakopoulou VA. (2005). Akt activation correlates with adverse outcome in tongue cancer. *Cancer* **104**: 2430-6.

Matsuda-Lennikov M, Suizu F, Hirata N, Hashimoto M, Kimura K, Nagamine T, Fujioka Y, Ohba Y, Iwanaga T, Noguchi M (2014). Lysosomal interaction of Akt with Phafin2: a critical step in the induction of autophagy. *PloS one* **9**: e79795.

Mehrpour M, Esclatine A, Beau I, Codogno P (2010). Overview of macroautophagy regulation in mammalian cells. *Cell Res* **20**: 748-62.

Mende I, Malstrom S, Tschlis PN, Vogt PK, Aoki M (2001). Oncogenic transformation induced by membrane-targeted Akt2 and Akt3. *Oncogene* **20**: 4419-23.

Mirza AM, Kohn AD, Roth RA, McMahon M (2000). Oncogenic transformation of cells by a conditionally active form of the protein kinase Akt/PKB. *Cell Growth Differ* **11**: 279–292.

Mourao RV, Junior EC, Barros Silva PG (2016). Study of the relationship between mononuclear inflammatory infiltrate and Ki-67 and basement membrane and extracellular matrix protein expression in radicular cysts. *49*: 447-53.

Nicholson KM, Anderson NG (2002). The protein kinase B/Akt signalling pathway in human malignancy. *Cellular signalling* **14**: 381-95.

Nicholson KM, Streuli CH, Anderson NG (2003). Autocrine signalling through erbB receptors promotes constitutive activation of protein kinase B/Akt in breast cancer cell lines. *Breast Cancer Res Treat* **81**: 117–128.

Noguchi M, Hirata N, Suizu F (2014). The links between AKT and two intracellular proteolytic cascades: ubiquitination and autophagy. *Biochimica et biophysica acta*. **1846**: 342-52.

Oleinik NV, Krupenko NI, Krupenko SA (2007). Cooperation between JNK1 and JNK2 in activation of p53 apoptotic pathway. *Oncogene* **26**: 7222-30.

Osuka S, Sampetean O, Shimizu T, Saga I, Onishi N, Sugihara E, Okubo J, Fujita S, Takano S, Matsumura A, Saya H. (2013). IGF1 receptor signaling regulates adaptive radioprotection in glioma stem cells. *Stem cells* **31**: 627-40.

Sun M, Wang G, Paciga JE, Feldman RI, Yuan ZQ, Ma XL, Shelley SA, Jove R, Tsihchlis PN, Nicosia SV, Cheng JQ (2001). AKT1/PKBa kinase is frequently elevated in human cancers and its constitutive activation is required for oncogenic transformation in NIH3T3 cells. *Am J Pathol* **159**: 431–437.

Tabor MP, Braakhuis BJ, van der Wal JE, van Diest PJ, Leemans CR, Brakenhoff RH, et al (2003). Comparative molecular and histological grading of epithelial dysplasia of the oral cavity and the oro pharynx. *J Pathol* **199**:354- 60.

Takamura A, Komatsu M, Hara T, Sakamoto A, Kishi C, Waguri S, Eishi Y, Hino O, Tanaka K, Mizushima N (2011). Autophagy-deficient mice develop multiple liver tumors. *Genes & development* **25**: 795-800.

Tenbaum SP, Ordonez-Moran P, Puig I, Chicote I, Arques O, Landolfi S, Fernández Y, Herance JR, Gispert JD, Mendizabal L, Aguilar S, Ramón y Cajal S, Schwartz S Jr, Vivancos A, Espín E, Rojas S, Baselga J, Tabernero J, Muñoz A, Palmer HG (2012). Beta-catenin confers resistance to PI3K and AKT inhibitors and subverts FOXO3a to promote metastasis in colon cancer. *Nature medicine* **18**: 892-901.

Ueno NT, Mamounas EP (2016). Neoadjuvant nab-paclitaxel in the treatment of breast cancer. *Breast Cancer Res Treat* **156**:427-40.

Van de Sande T, Roskams T, Lerut E, Joniau S, Van Poppel H, Verhoeven G, Swinnen JV (2005). High-level expression of fatty acid synthase in human prostate cancer tissues is linked to activation and nuclear localization of Akt/PKB. *J Pathol* **206**: 214–219.

Van der Heide LP, Hoekman MF, Smidt MP (2004). The ins and outs of FoxO shuttling: mechanisms of FoxO translocation and transcriptional regulation. *The Biochemical journal* **380**: 297-309.

Vasconcelos MG, Vasconcelos RG, Oliveira DHIP, Santos EM, Silveira EJD, Queiroz LMG (2015). Distribution of Hypoxia-Inducible Factor-1a and Glucose Transporter-1 in Human Tongue Cancers. *J Oral Maxillofac Surg* **73**: 1753-1760.

Vasko V, Saji M, Hardy E, Kruhlak M, Larin A, Savchenko V, Miyakawa M, Isozaki O, Murakami H, Tsushima T, Burman KD, De Micco C, Ringel MD (2004), Akt activation and localization correlate with tumour invasion and oncogene expression in thyroid cancer. *J Med Genet* **41**: 161–170.

Wagner EF, Nebreda AR (2009). Signal integration by JNK and p38 MAPK pathways in cancer development. *Nature reviews Cancer* **9**: 537-49.

Wang H, Yang YB, Shen HM, Gu J, Li T, Li XM (2012). ABT-737 induces Bim expression via JNK signaling pathway and its effect on the radiation sensitivity of HeLa cells. *PLoS one* **7**: e52483.

Warnakulasuriya S, Reibel J, Bouquot J, Dabelsteen E (2008). Oral epithelial dysplasia classification systems: predictive value, utility, weaknesses and scope for improvement. *Journal of oral pathology & medicine: official publication of the International Association of Oral Pathologists and the American Academy of Oral Pathology* **37**: 127-33.

West KA, Castillo SS, Dennis PA (2002). Activation of the PI3K/Akt pathway and chemotherapeutic resistance. *Drug resistance updates: reviews and commentaries in antimicrobial and anticancer chemotherapy* **5**: 234-48.

Vieira FL, Vieira BJ, Guimaraes MA, Aarestrup FM (2008). Cellular profile of the peritumoral inflammatory infiltrate in squamous cells carcinoma of oral mucosa: Correlation with the expression of Ki67 and histologic grading. *BMC Oral Health* **8**: 25.

Xie X, Zhang D, Zhao B, Lu MK, You M, Condorelli G, Wang CY, Guan KL (2011). I $\kappa$ B kinase epsilon and TANK-binding kinase 1 activate AKT by direct phosphorylation. *Proc Natl Acad Sci* **108**: 6474–6479.

Yu S, Yu Y, Zhang W, Yuan W, Zhao N, Li Q, Cui Y, Wang Y, Li W, Sun Y, Liu T (2016). FOXO3a promotes gastric cancer cell migration and invasion through the induction of cathepsin L. *Oncotarget* [Epub ahead of print]

Yu Z, Weinberger PM, Sasaki C, Egleston BL, Speier WF, Haffty B, Kowalski D, Camp R, Rimm D, Vairaktaris E, Burtness B, Psyrri A (2007). Phosphorylation of Akt (Ser473) Predicts Poor Clinical Outcome in Oropharyngeal Squamous Cell Cancer. *Cancer Epidemiol Biomarkers Prev* **16**: 553-558

Zhou J, Xu G, Ma S, Li F, Yuan M, Xu H, Huang K (2015). Catalpol ameliorates high-fat diet-induced insulin resistance and adipose tissue inflammation by suppressing the JNK and NF- $\kappa$ B pathways. *Biochem Biophys Res Commun* **467**: 853-8.

## FIGURES

**Figure 1.** P-Akt immunoreactivity was found in the membrane, cytoplasm, nucleus and perinucleus of malignant cells. In the NOE (B1), there was a weak cytoplasmic staining (arrow) and absence of immunoreactivity of p-AKT membrane (higher magnification). In OED we found a bigger and stronger cytoplasmic immunostaining as it takes the high-risk classification (higher magnification) and observed a prevalence of moderate cytoplasmic immunostaining in B2 (arrow) and a greater prevalence of strong cytoplasmic immunostaining in B3 (arrow). Immunoreactivity of P-AKT was most observed in the membrane, cytoplasm, nucleus and perinuclear region of OSCC cells (higher magnification in B4 and B5). In B4 it is shown a higher perinuclear marking (arrow) and in B5 it is observed higher nuclear staining (arrow). P-JNK immunoreactivity was found in the nucleus and cytoplasm of OSCC, OED and NOE. There was a higher strong nuclear immunostaining directly associated with the gradation control (C1) to OED (C2 and C3) and OSCC (C4 and C5), in C1 we observed a predominance of strong nuclear staining (greater magnification and arrow) while in C4 further weak nuclear immunostaining is more evident (greater magnification and arrow). nuclear P-JNK expression in OSCC appears to be lost to the malignant transformation of the lesion advances. FOXO3a immunoreactivity was found in the nucleus and cytoplasm of malignant, dysplastic and NOE cells. The loss of Nuclear expression in FOXO3a looks similar to the patterns observed in p-JNK, showing a predominance of strong nuclear staining in D1 (arrow), moderate and weak nuclear staining in D2 and D3 (greater magnification and arrow). Nuclear marking absence was more observed in OSCC (higher magnification D4 and D5). Greater cytoplasmic staining was observed in OSCC with the weak cytoplasmic labeling in D4 and and the moderate in D5 (arrow and higher magnification). The Ki-67 immunoreactivity was found in the nucleoplasm and the nucleolus of malignant cells (higher magnification and arrows and E4 and E5), and in NOE immunostaining was restricted to basal and parabasal layers epithelial layers (E1). The intensity and number of Ki-67 immunostained cells increases with progression of the malignant disease cells.

**Figure 2.** Path diagram depicting the covariance structure model of OSCC immunostaining profile. Rectangles represent manifest (measured) variables. Single-headed arrows represent correlations between the immunostaining patterns. Numbers adjacent to arrows are standardized path coefficients. Variables on the left are assumed to be causally prior to those on the right. \*,  $P < 0.05$ ; \*\*,  $P < 0.01$ ; \*\*\*,  $P < 0.001$ .

**Figure 3.** Path diagram depicting the covariance structure model of Oral Epithelial Dysplasias immunostaining profile. Rectangles represent manifest (measured) variables. Single-headed arrows represent the correlations between the immunostaining patterns. Numbers adjacent to arrows are standardized path coefficients. Variables on the left are assumed to be causally prior to those on the right. \*,  $P < 0.05$ ; \*\*,  $P < 0.01$ ; \*\*\*,  $P < 0.001$ .

## TABLES

**Table 1.** Antibody specifications

<b>Antibody</b>	<b>Specification</b>	<b>Flask / concentration</b>	<b>Brand</b>	<b>Positive Control</b>	<b>Dilution</b>	<b>Incubation Time</b>	<b>Antigenic Retrieval Method</b>
<b>Anti-AKT1 (phospho S473)</b>	Rabbit mono ab - clone EP2109Y	100g	Abcam	Cervical cancer	1:100	Overnight	Trylogy ph6
<b>Anti-JNK1 + JNK2 + JNK3 (phospho T183+T 183+T221)</b>	Rabbit mono ab - clone EPR5693	100g / 100 µl / 1.071 - 1.732 mg/ml	Abcam	Brain	1:100	2 hours	Citrate ph6
<b>Anti-FoxO3A</b>	Rabbit poli ab	100g / 50 µl / 1.1 - 1.12 mg/ml	Abcam	Cervical cancer	1:100 (OSCC) 1:400 (OED)	60 min	Citrate ph6
<b>Ki-67</b>	Rabbit mono ab	100 µg / 0.9 - 1 mg/ml	Abcam	Lymph node	1:300	Overnight	Citrate ph6

**Table 2:** Mean and intensity of immunostained cells in membrane, cytoplasm and nucleus of oral epithelial dysplasia and oral squamous cell carcinoma.

Antibody/Staining	cells			p
	NOE	OED	OSCC	
p-AKT - nuclear	1.8±4.7	7.9±8.1	21.2±19.0* <sup>†</sup>	<b>0.002</b>
p-AKT - perinuclear	14.3±8.1	20.2±10.0	15.1±9.5	0.181
p-AKT - strong cytoplasmic	14.9±7.6	16.1±11.0	8.2±6.8*	<b>0.022</b>
p-AKT - moderate cytoplasmic	44.8±9.5	35.8±8.4	28.2±12.3*	<b>0.002</b>
p-AKT - weak cytoplasmic	39.5±10.9	42.8±12.3	59.9±15.7* <sup>†</sup>	<b>&lt;0.001</b>
p-AKT - negative cytoplasmic	0.8±0.6	5.2±4.6*	6.1±5.5*	<b>0.032</b>
p-AKT - strong membrane	0.0±0.0	10.1±10.3	17.7±19.7*	<b>0.025</b>
p-AKT - moderate membrane	0.0±0.0	20.0±12.2*	18.9±11.9*	<b>0.001</b>
p-AKT - weak membrane	0.0±0.0	19.3±7.8*	52.6±21.7* <sup>†</sup>	<b>&lt;0.001</b>
p-AKT - negative membrane	100.0±0.0	50.6±23.7*	33.9±20.8* <sup>†</sup>	<b>&lt;0.001</b>
Ki67 - strong nuclear	1.9±2.0	11.8±10.6	48.1±49.6* <sup>†</sup>	<b>&lt;0.001</b>
Ki67 - weak nuclear	8.6±3.1	13.3±3.9*	16.3±4.8*	<b>&lt;0.001</b>
Ki67 - moderate nuclear	3.3±1.2	7.3±3.2	20.2±7.4* <sup>†</sup>	<b>&lt;0.001</b>
Ki67 - nuclear	12.3±4.1	25.8±9.1*	54.6±16.8* <sup>†</sup>	<b>&lt;0.001</b>
p-JNK - strong nuclear	48.3±13.7	11.0±10.3*	1.1±1.3* <sup>†</sup>	<b>&lt;0.001</b>
p-JNK - weak nuclear	9.9±7.6	32.5±12.0*	49.8±19.5* <sup>†</sup>	<b>&lt;0.001</b>
p-JNK - moderate nuclear	14.4±10.8	19.7±15.5	17.7±20.5	0.844
p-JNK - negative nuclear	27.5±13.0	36.9±18.4	31.4±14.3	0.421
p-JNK - strong cytoplasmic	0.1±0.3	0.4±0.4	0.9±1.0	0.090
p-JNK - weak cytoplasmic	21.5±42.0	25.0±24.5	17.4±16.5	0.587
p-JNK - moderate cytoplasmic	0.2±0.4	2.2±3.6	1.8±1.8	0.402
p-JNK - negative cytoplasmic	78.2±41.8	72.3±26.7	80.0±16.7	0.606
FoxO3a - strong nuclear	13.5±4.8	3.2±5.4*	0.0±0.1* <sup>†</sup>	<b>&lt;0.001</b>
FoxO3a - weak nuclear	8.8±2.6	15.6±11.9*	3.3±3.8* <sup>††</sup>	<b>&lt;0.001</b>
FoxO3a - moderate nuclear	68.6±10.7	15.8±16.9*	0.6±0.8* <sup>†</sup>	<b>&lt;0.001</b>
FoxO3a - negative nuclear	9.1±3.6	65.4±25.4*	96.1±4.3* <sup>†</sup>	<b>&lt;0.001</b>
FoxO3a - strong cytoplasmic	0.0±0.0	19.5±32.7	5.0±14.4	0.102
FoxO3a - weak cytoplasmic	10.0±13.8	19.7±16.9*	41.6±27.0* <sup>†</sup>	<b>0.002</b>
FoxO3a - moderate cytoplasmic	83.5±10.6	35.4±36.4*	46.4±28.4	<b>0.014</b>
FoxO3a - negative cytoplasmic	6.5±4.9	25.3±28.6	7.0±8.8 <sup>†</sup>	<b>0.015</b>

NOE: normal oral epithelium; OED: oral epithelial dysplasia; OSCC: oral squamous cell carcinoma  
 \*p<0.05 versus NOE, <sup>†</sup>p<0.05 versus OED, Text ANOVA/Bonferroni (media ± DP).

**Table 3:** Mean and intensity of immunostained cells in membrane, cytoplasm and nucleus of low and high-risk oral epithelial dysplasia.

Antibody/Staining	OED		<i>p</i>
	Low Risk	High Risk	
p-AKT - nuclear	9.71±9.58	6.11±6.25	0.333
p-AKT - perinuclear	25.10±8.06	15.25±9.55	<b>0.022</b>
p-AKT - strong cytoplasmic	15.93±10.59	16.36±11.91	0.933
p-AKT - moderate cytoplasmic	34.12±5.75	37.50±10.41	0.384
p-AKT - weak cytoplasmic	45.60±13.01	40.01±11.43	0.321
p-AKT - negative cytoplasmic	4.4±2.8	6.1±5.5	0.407
p-AKT - strong membrane	3.33±4.37	16.92±10.09	<b>0.002</b>
p-AKT - moderate membrane	11.60±8.06	28.33±9.64	<b>0.001</b>
p-AKT - weak membrane	17.65±4.96	20.87±9.91	0.375
p-AKT - negative membrane	67.4±11.3	33.9±20.8	<b>&lt;0.001</b>
Ki67 - strong nuclear	8.30±7.51	15.33±12.38	0.142
Ki67 - weak nuclear	12.26±3.68	14.32±4.02	0.247
Ki67 - moderate nuclear	6.87±3.87	7.81±2.57	0.530
Ki67 - nuclear	23.79±9.76	27.77±8.34	0.340
p-JNK - strong nuclear	15.47±11.33	6.50±7.25	<b>0.049</b>
p-JNK - weak nuclear	29.35±11.01	35.59±12.61	0.254
p-JNK - moderate nuclear	22.17±14.07	17.14±17.16	0.483
p-JNK - negative nuclear	33.03±15.50	40.78±20.99	0.360
p-JNK - strong cytoplasmic	0.32±0.28	0.51±0.47	0.286
p-JNK - weak cytoplasmic	25.37±23.37	24.67±26.87	0.951
p-JNK - moderate cytoplasmic	2.09±3.19	2.39±4.20	0.859
p-JNK - negative cytoplasmic	72.22±25.85	72.46±28.87	0.985
FoxO3a - strong nuclear	4.39±6.50	1.96±4.04	0.331
FoxO3a - weak nuclear	21.25±12.03	9.98±9.02	<b>0.029</b>
FoxO3a - moderate nuclear	22.83±13.08	8.76±18.02	0.061
FoxO3a - negative nuclear	51.51±15.00	79.28±26.71	<b>0.010</b>
FoxO3a - strong cytoplasmic	18.58±30.69	20.51±36.24	0.899
FoxO3a - weak cytoplasmic	29.12±18.39	10.33±8.28	<b>0.012</b>
FoxO3a - moderate cytoplasmic	26.87±26.80	43.89±43.81	0.311
FoxO3a - negative cytoplasmic	25.42±22.42	25.27±35.00	0.991

OED: oral epithelial dysplasia

\**p*<0.05, Test t de Student (media ± DP).



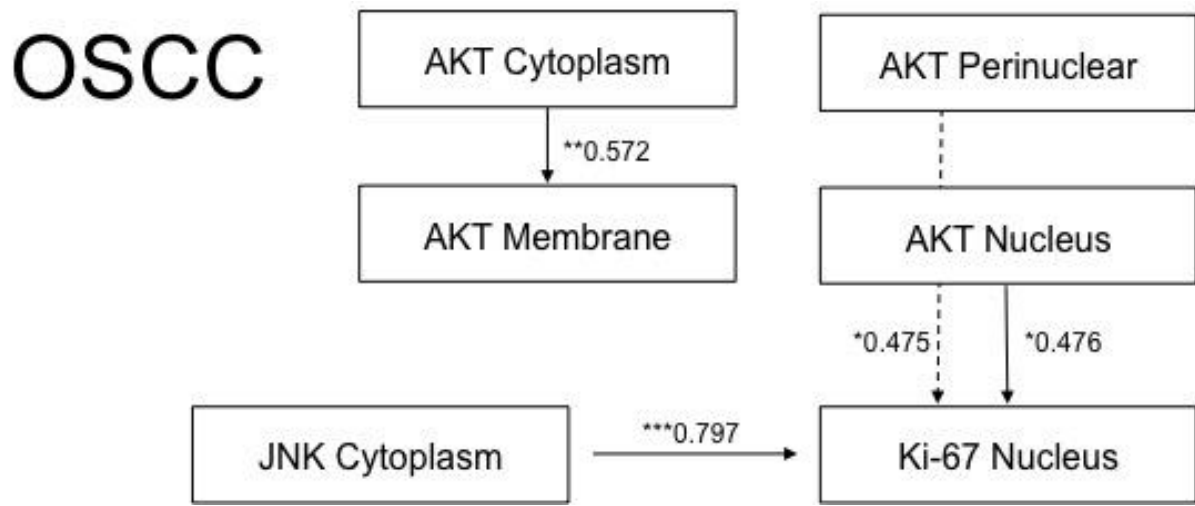
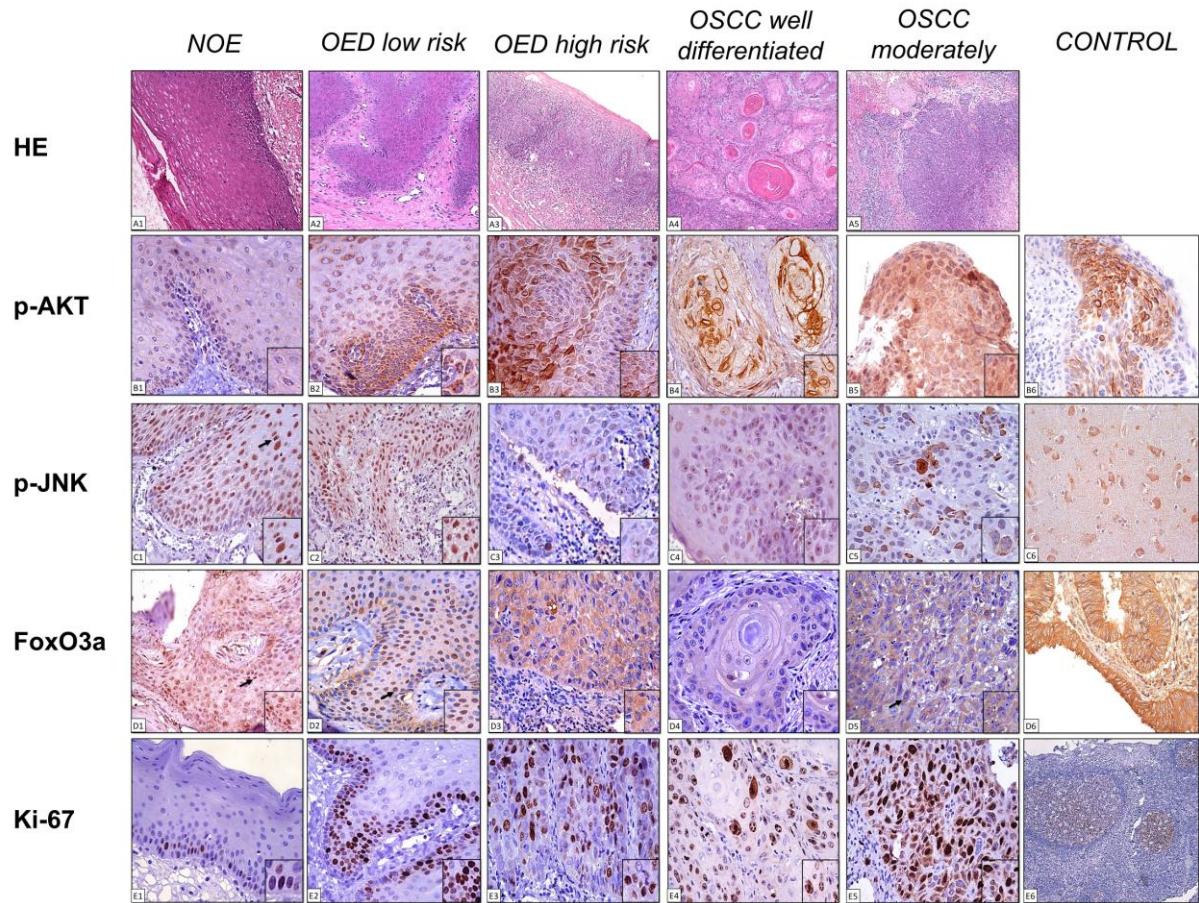
**Table 4:** Mean and intensity of immunostained cells in membrane, cytoplasm and nucleus of low and high-risk oral epithelial dysplasia and oral squamous cell carcinoma.

Antibody/Staining	NOE	OED		OSCC	p
		Low Risk	High Risk		
p-AKT - nuclear	1.8±4.7	9.71±9.58	6.11±6.25	21.2±19.0*†‡	<b>0.005</b>
p-AKT - perinuclear	14.3±8.1	25.10±8.06	15.25±9.55	15.1±9.5†	<b>0.029</b>
p-AKT - strong cytoplasmic	14.9±7.6	15.93±10.59	16.36±11.91	8.2±6.8	0.055
p-AKT - moderate cytoplasmic	44.8±9.5	34.12±5.75	37.50±10.41	28.2±12.3*	<b>0.005</b>
p-AKT - weak cytoplasmic	39.5±10.9	45.60±13.01	40.01±11.43	59.9±15.7*‡	<b>0.001</b>
p-AKT - negative cytoplasmic	0.8±0.6	4.4±2.8	6.1±5.5*	3.7±3.3	<b>0.047</b>
p-AKT - strong membrane	0.0±0.0	3.33±4.37	16.92±10.09	17.7±19.7*	<b>0.008</b>
p-AKT - moderate membrane	0.0±0.0	11.60±8.06	28.33±9.64*†	18.9±11.9*	<b>&lt;0.001</b>
p-AKT - weak membrane	0.0±0.0	17.65±4.96	20.87±9.91*	52.6±21.7*†‡	<b>&lt;0.001</b>
p-AKT - negative membrane	100.0±0.0	67.4±11.3*	33.9±20.8*†	10.8±11.5*†‡	<b>&lt;0.001</b>
Ki67 - strong nuclear	1.9±2.0	8.30±7.51	15.33±12.38	48.1±49.6*†	<b>0.001</b>
Ki67 - weak nuclear	8.6±3.1	12.26±3.68	14.32±4.02*	16.3±4.8*	<b>&lt;0.001</b>
Ki67 - moderate nuclear	3.3±1.2	6.87±3.87	7.81±2.57	20.2±7.4*†‡	<b>&lt;0.001</b>
Ki67 - nuclear	12.3±4.1	23.79±9.76	27.77±8.34*	54.6±16.8*†‡	<b>&lt;0.001</b>
p-JNK - strong nuclear	48.3±13.7	15.47±11.33*	6.50±7.25*	1.1±1.3*†	<b>&lt;0.001</b>
p-JNK - weak nuclear	9.9±7.6	29.35±11.01	35.59±12.61	49.8±19.5*†	<b>&lt;0.001</b>
p-JNK - moderate nuclear	14.4±10.8	22.17±14.07	17.14±17.16	17.7±20.5	0.865
p-JNK - negative nuclear	27.5±13.0	33.03±15.50	40.78±20.99	31.4±14.3	0.415
p-JNK - strong cytoplasmic	0.1±0.3	0.32±0.28	0.51±0.47	0.9±1.0	0.166
p-JNK - weak cytoplasmic	21.5±42.0	25.37±23.37	24.67±26.87	17.4±16.5	0.787
p-JNK - moderate cytoplasmic	0.2±0.4	2.09±3.19	2.39±4.20	1.8±1.8	0.602
p-JNK - negative cytoplasmic	78.2±41.8	72.22±25.85	72.46±28.87	80.0±16.7	0.804
FoxO3a - strong nuclear	13.5±4.8	4.39±6.50*	1.96±4.04*	0.0±0.1*†	<b>&lt;0.001</b>
FoxO3a - weak nuclear	8.8±2.6	21.25±12.03*	9.98±9.02	3.3±3.8*†	<b>&lt;0.001</b>
FoxO3a - moderate nuclear	68.6±10.7	22.83±13.08*	8.76±18.02*†	0.6±0.8*†	<b>&lt;0.001</b>
FoxO3a - negative nuclear	9.1±3.6	51.51±15.00*	79.28±26.71*†	96.1±4.3*†‡	<b>&lt;0.001</b>
FoxO3a - strong cytoplasmic	0.0±0.0	18.58±30.69	20.51±36.24	5.0±14.4	0.208
FoxO3a - weak cytoplasmic	10.0±13.8	29.12±18.39	10.33±8.28	41.6±27.0*‡	<b>0.001</b>
FoxO3a - moderate cytoplasmic	83.5±10.6	26.87±26.80*	43.89±43.81	46.4±28.4	<b>0.019</b>
FoxO3a - negative cytoplasmic	6.5±4.9	25.42±22.42*	25.27±35.00*	7.0±8.8	<b>0.040</b>

NOE: normal oral epithelium; OED: oral epithelial dysplasia; OSCC: oral squamous cell carcinoma

\*p<0.05 versus NOE, †p<0.05 versus Low Risk OED, ‡p<0.05 versus High Risk OED;

Test ANOVA/Bonferroni (media ± DP).



OED

